Journal of the European Ceramic Society 20 (2000) 2641–2648

Interfacial and thermomechanical characterization of reaction formed joints in silicon carbide-based materials

J. Martínez Fernández [a,*], A. Muñoz [a], F.M. Varela-Feria [a], M. Singh [b]

[a] *Departamento de Física de la Materia Condensada, Universidad de Sevilla, Apdo. 1065, Seville, Spain*
[b] *NASA Glenn Research Center, Ceramics Branch, MS106-5, Cleveland, OH 44135, USA*

Received 8 March 2000; received in revised form 29 April 2000; accepted 11 May 2000

Abstract

The microstructure and mechanical properties of reaction formed joints of Refel™ reaction bonded SiC (RB-SiC) and Hexoloy™ sintered SiC were studied in order to achieve a better understanding of the influence of base materials and joining process parameters on the high temperature strength of reaction formed joints. Transmission electron microscopy (TEM), scanning electron microscopy (SEM), and optical microscopy were used to characterize the joints prior to mechanical tests. The microstructural analysis indicated that the joints consist of silicon carbide (SiC) grains (with grain sizes ranging from 0.1 to 2 μm) and crystalline silicon as an intergranular phase. Most of the silicon carbide grains in the joint have hexagonal crystal structure with certain preferential orientations related to the silicon matrix. The high temperature strength of joints was measured by constant strain rate experiments in compression where joints were forming 45° with the compression axe. The strength of the joined Refel RB-SiC has been found to be at least equal to that of the bulk materials (550 MPa at 1235°C and 400 MPa at 1385°C). The joined Hexoloy specimens had strengths (1.4 GPa at 1290°C and 750 MPa at 1420°C) lower than the bulk material but higher than the joints of RB-SiC.

Keywords: Interfaces; Joining; Mechanical properties; Microstructure-final; SiC

1. Introduction

In recent years, there has been a surge of interest in the research, development, and testing of silicon carbide-based monolithic ceramic and composite components for a number of aerospace and ground-based systems. The engineering design often requires fabrication and manufacturing of complex shaped components, which are quite expensive. In many instances, it is much more economical to build up complex shapes by joining together geometrically simple shapes. However, the joints must have good mechanical strength and environmental stability comparable to the bulk materials. In addition, the joining technique should be practical, and reliable.

The majority of the techniques used today are based on the joining of monolithic ceramics with metals either by diffusion bonding, metal brazing, brazing with oxides and oxynitrides, or diffusion and friction welding.[1–3] The joints produced by these techniques require either high temperatures for processing or hot pressing (high pressures) and have different thermal expansion coefficients than the parent materials. In order to obtain ceramic joints with high temperature capability, ceramic joint interlayers have been produced via pre-ceramic polymers, in-situ displacement reactions, and tape casting/reaction bonding techniques.[3–5] These ceramic joints have certain limitations related with the significant amounts of porosity, low strength, and/or poor control of the joint microstructure.

The reaction forming technique reported here is unique in terms of producing joints with tailorable microstructure and properties. Fabrication of joints by this approach is attractive since the thermomechanical properties of the joint interlayer can be tailored to be very close to those of the silicon carbide based materials. In addition, high temperature fixturing is not needed to hold the parts at the infiltration temperature. A wide variety of silicon carbide-based ceramics (reaction bonded, sintered, CVD, etc.) and fiber reinforced composites have been joined using this approach.[6–14] In

* Corresponding author.
E-mail address: martinez@cica.es (J. Martínez Fernández).

0955-2219/00/$ - see front matter
PII: S0955-2219(00)00156-4

previous studies, flexure tests were used to characterize the room and high temperature mechanical properties of joints in monolithic silicon carbide-based materials.[10,11,15] However, these joints are expected to encounter various types of stress conditions. In order to obtain detailed information of the mechanical behavior, it became apparent to use a test where the imposed stress and the strain rate can be directly measured. There is also a need for compressive and shear strength data of joints that can not be provided by the flexural tests.

In this paper, the microstructure and compressive mechanical properties of reaction formed joints in Refel™ RB-SiC and Hexoloy™ sintered SiC materials are presented. Optical, scanning and transmission electron microscopy have been used to characterize the joint microstructure. The high temperature compressive strength of joints (scarf butt geometry) has been measured up to 1420°C in air. The test specimen geometry requires a small amount of material and the stress and strain can be directly measured. The compressive strength of joints has been compared to that of bulk material.

2. Experimental procedures

The RB-SiC and sintered SiC materials used in this study were provided by Pure Carbon Co., PA, USA and Carborundum Co., Niagara Falls, NY, USA, respectively. Refel™ (RB-SiC) materials were fabricated by the reaction bonding of coarse and fine silicon carbide grains with silicon using a liquid silicon infiltration process. Hexoloy™ materials were fabricated by sintering of alpha-SiC. As-processed samples were sectioned, mounted, and polished for metallographic studies. For joining studies, 6×3 cm size silicon carbide pieces were machined from SiC plates. These pieces were cleaned in acetone and dried.

Experimental details of the joining process have been given in other publications.[6–14] The joining steps include the application of a carbonaceous mixture in the joint area and curing at 110–120°C for 10 to 20 min. Silicon in paste form is applied in the joint region and heated up to 1425°C for 5–10 min. The molten silicon reacts with carbon to form silicon carbide with controllable amounts of silicon. The silicon content of the joint was measured from optical micrographs using a semiautomatic image analyzer (Videoplan, Kontron Electronik).

TEM specimens were cut from the joined samples and thinned to electron transparency using standard techniques. Special care was taken to ensure that the thinned region contained part of the joint. Microstructural observations were performed using a Philips CM200 electron microscope operating at 200 kV (Electron Microscopy Service, Seville, Spain).

For mechanical property measurements, small parallelepipeds of 2.3×2.3×4 mm were machined from the large specimen. The specimens were tested in compression at a constant strain rate of 2×10^{-5} s^{-1} for temperatures ranging from 1235 to 1420°C, in air. Testing was performed using a screw driven Instron universal testing machine model 1185 with a furnace mounted on its frame. Alumina rods with SiC pads were used. The load/time behavior was monitored on a chart recorder. The specimen geometry is shown in Fig. 1 where the joint is at a 45° angle with the compression axis.

3. Results

3.1. Microstructural characterization

The microstructure of the as-received RB-SiC is composed of very large α-SiC grains (with sizes up to 30 μm), and considerably smaller grains (with sizes ranging from 1 to 5 μm). The large SiC grains have a very uniform crystalline structure without many stacking faults and other defects. The small grains are perfectly adapted to the grain boundary of the large grains, and other areas are filled by silicon (the volume fraction of silicon is 10.5±0.8%).

The sintered SiC is composed of α-SiC grains with sizes ranging from 0.5 to 5 μm. The grains have hexagonal crystal structure and stacking faults are very common. Pores in triple points were frequently found. These pores are due to incomplete sintering and are not due to preferential thinning because they are also observed by optical microscopy.[10,11]

The typical microstructure of the joints is shown in Fig. 2. The white and gray areas are Si and SiC, respectively. The silicon is finely distributed in regions

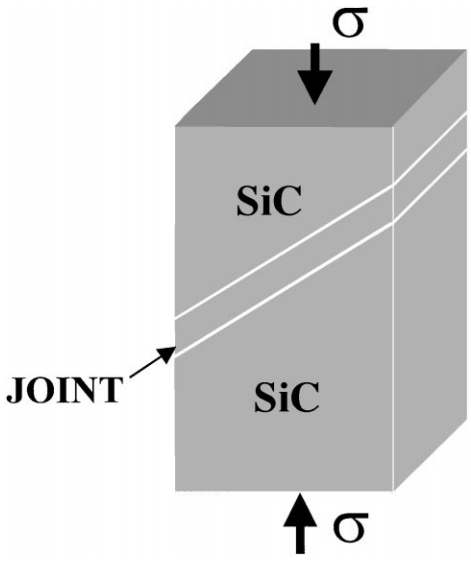

Fig. 1. Test geometry.

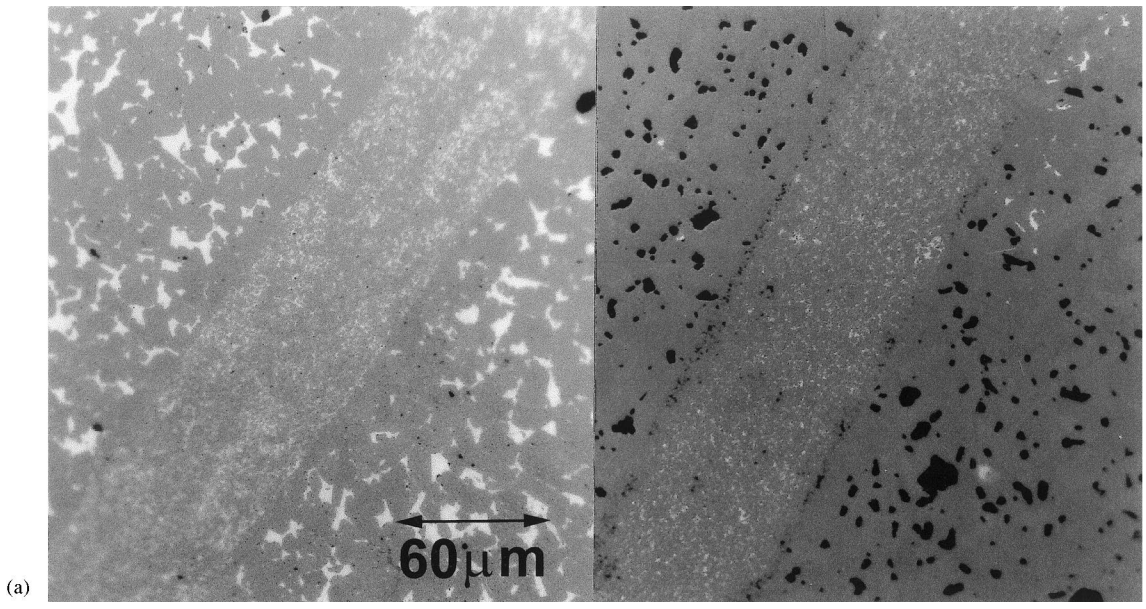

(a) (b)

Fig. 2. Optical micrograph of the undeformed joint: (left) RB-SiC; (right) Sintered SiC.

of approximately the same size as the SiC areas. The silicon areas are clearly smaller in the joint than in the RB-SiC (Fig. 2a) and about the same size as the triple points in the sintered SiC (Fig. 2b). The joint thickness for the RB-SiC and sintered SiC were 58.2±1.2 μm and 63.1±0.6 μm respectively. The volume fraction of silicon in the joint was 7.3±2.2%.

In Fig. 3, TEM micrographs of the SiC/joint interphase in RB-SiC and sintered SiC are shown. In both materials, the interphase is very sharp and does not show any evidence of cracks or other macroscopic defects. Sometimes dislocation networks were observed next to the interphase. Si/SiC, Si/Si or SiC/SiC interfaces were found forming the SiC-joint interphase, although the first one seemed to be more predominant.

In Fig. 4a, a micrograph of the joint microstructure is shown. The microstructure of the joint was similar for both types of joined materials. The grain size was 0.85 0.70 μm with most of the grains ranging from 0.1 to 0.5 μm, and with some grains with sizes up to 2 μm. Fig. 4b shows a detail of the joint where the matrix between grains can be observed. This matrix is crystalline Si, as can be deduced from the diffraction patterns shown as an insert on Fig. 4b, where the matrix is oriented on the [112] (left) and [011] (right) zone axis.

Most of the grains inside the joint were α-SiC. Fig. 5a shows an α-SiC grain oriented on the [0001] zone axis (the diffraction pattern is shown as an insert). In this orientation, different hexagonal polytypes can not be differentiated. It is common to observe SiC grains in the joint with similar orientations. For example, without tilting the specimen from the situation of Fig. 5a, the grain shown in Fig. 5b, is also oriented on the [0001] zone axis, as many others (the diffraction pattern is

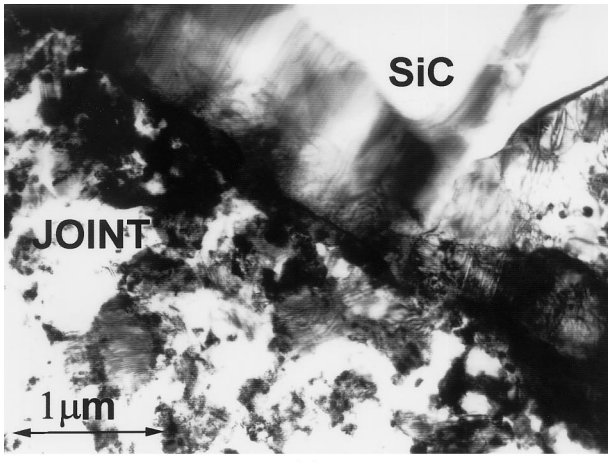

(a)

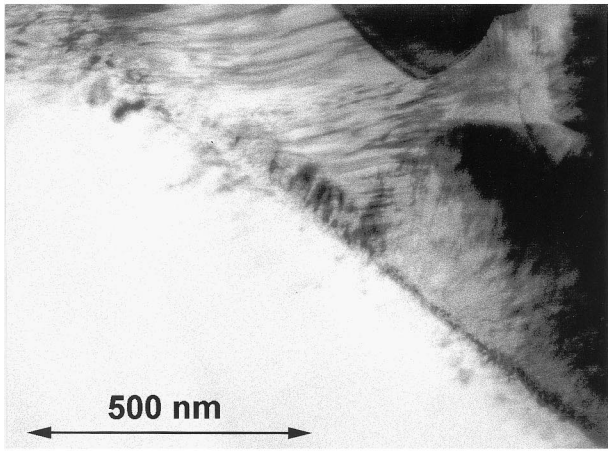

(b)

Fig. 3. (a) TEM micrograph of the interphase RB-SiC joint; (b) TEM micrograph of the interphase sintered SiC joint.

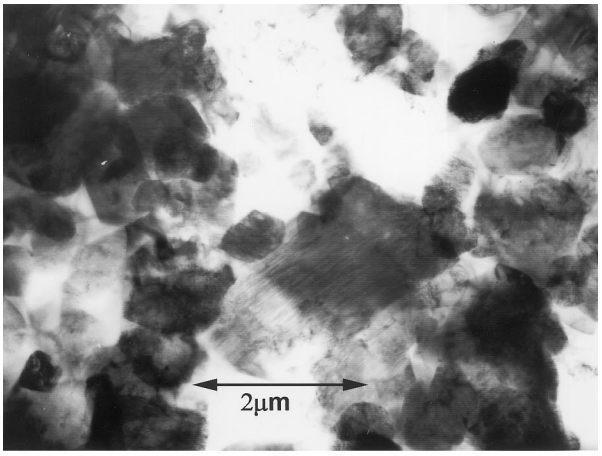

(a)

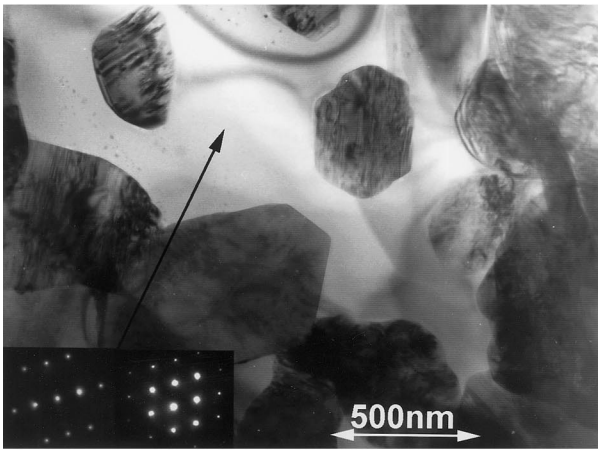

(b)

Fig. 4. (a) TEM micrograph of the joint microstructure; (b) detail of the joint microstructure. Diffraction patterns of the Si matrix included as an insert ([112] zone axis on the left, and [110] zone axis on the right).

shown as an insert). It must be noted that the diffraction patterns from Fig. 5a and b are rotated around the [0001] axis. Cubic β-SiC grains as the one shown in Fig. 5c (with the diffraction pattern, for the same orientation of Fig. 5a and b, also included) were also found. It is interesting to note that the β-SiC grain of Fig. 5c is also oriented in a low index ([112]) zone axis.

The orientation of the matrix was checked at different points and was found to be the same in large regions compared with the SiC grain size. For the orientation of the foil of Fig. 5a–c, the matrix was not oriented in a low index plane. The orientation of the matrix was indicated by the Kikuchi lines diagram showed in Fig. 5d. The matrix was oriented between [112], [114], and [125] zone axis, at approximately the same angle from the three of them. The preferential relationships between the Si and the SiC grains are controlled by a minimization of the interfacial energy, being this the reason for the similar orientation found on the SiC grains.

3.2. Mechanical characterization

The stress–strain curves obtained during the constant strain rate compressive experiments are shown in Fig 6. The joints of RB-SiC can undergo significant plastic deformation (the total strain prior to failure is over 10%), but in the joints of sintered SiC the plastic deformation is very small and probably occurring only in the joint itself (the total strain prior to failure is 4–5%). The strength [taken as the maximum stress held by the sample (Fig. 7)] decreases with temperature, but not dramatically. In the case of joints of sintered SiC, the strength is about 750 MPa, for temperatures over the melting point of silicon. The strength of the joints in RB-SiC is about the same as that of the bulk material. The joints of sintered SiC presented a strength significantly lower than the monolithic material but between two or three times larger than in RB-SiC.

After testing, samples were examined by SEM and optical microscopy. The joints of RB-SiC deformed uniformly at 1235 and 1335°C (Fig. 8a), the fracture plane often being perpendicular to the joint plane (arrowed in Fig. 8a). At the highest testing temperature used for RB-SiC (1385°C), silicon was observed on the sample surface and the deformation in the joint occurred mainly by shear. The geometry of deformation of the sintered SiC sample was different; the deformation and fracture only occurred on the joint for all temperatures, the two sintered SiC parts being unaltered (Fig. 8b). A closer look at the fracture surface shows that the joint fails internally and not at the joint-sintered SiC interphase.

4. Discussion

The compressive behavior and the geometry of deformation of the joined SiC depends on the relative strength of the joint and the material joined, the interphase between the joint and the bulk, and the microstructure and phase distribution of the joint. In the case of the joints in RB-SiC, the joint and the bulk material have a similar type of fabrication process in which some silicon remains as the intergranular phase (RB-SiC having larger grains and larger amount of silicon). Due to this similarity the joined sample deforms homogeneously, as if it did not have the joint (Fig. 8a). The failure does not occur along the joint and the joint is as strong or even stronger than the RB-SiC. The latter could be the case as the fracture occurs at 45° of the compressive axis (where the resolved shear stress is maximum) but in the plane perpendicular to the joint (arrowed in Fig. 8a and at higher magnification in Fig. 8c). The low amount of silicon in the joint, its crystallinity, and the interconnectivity of the SiC phase are key factors in good joint strengths. On the other hand,

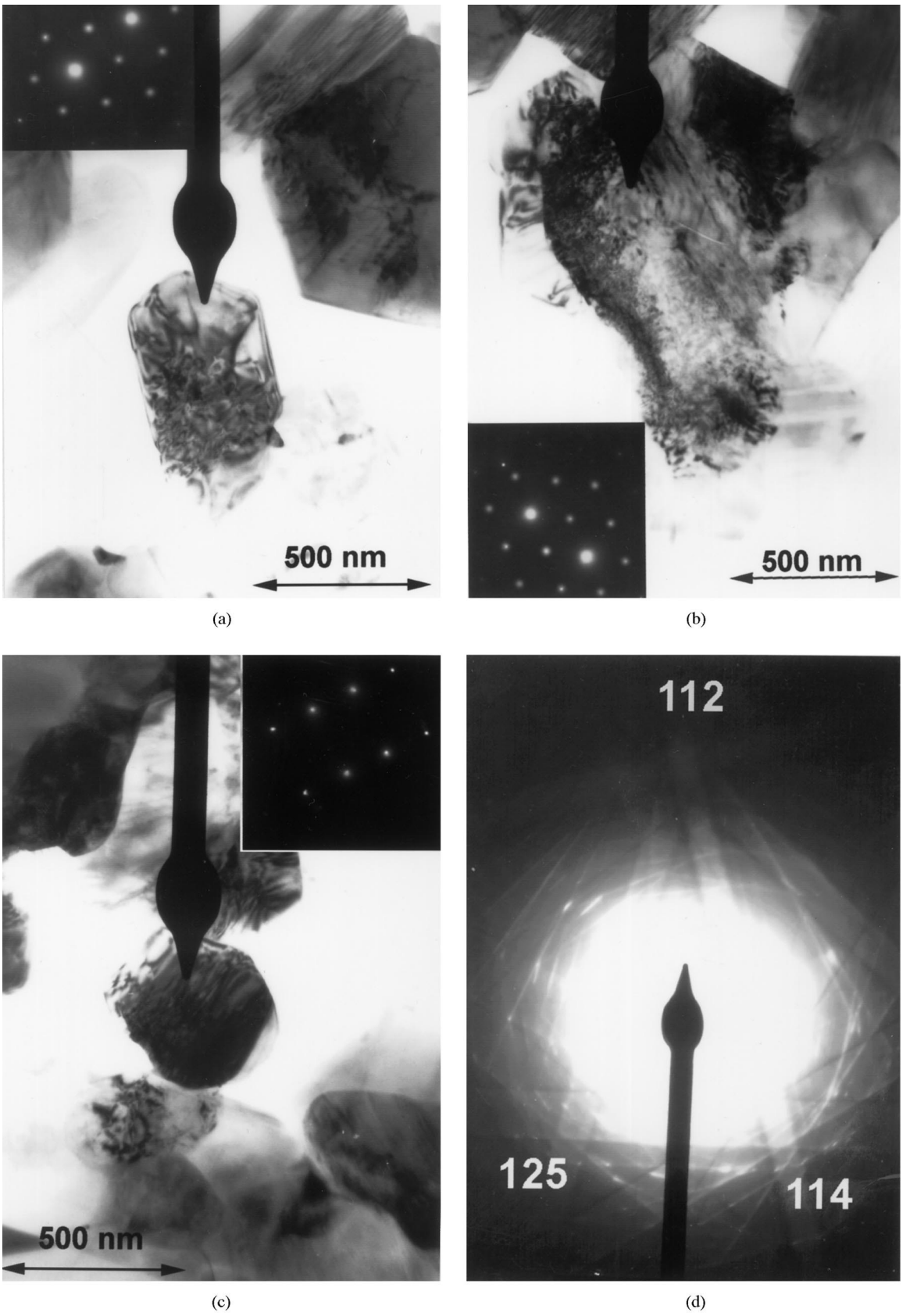

Fig. 5. (a)–(c) SiC grains of the joint with their respective diffraction patterns as an insert (for the same foil orientation); (d) Kikuchi line pattern of the Si matrix for the same orientation of patterns (a)–(c). The beam stop was used to indicate the SiC grains where the diffraction pattern was taken from and to make the Kikuchi lines more clear.

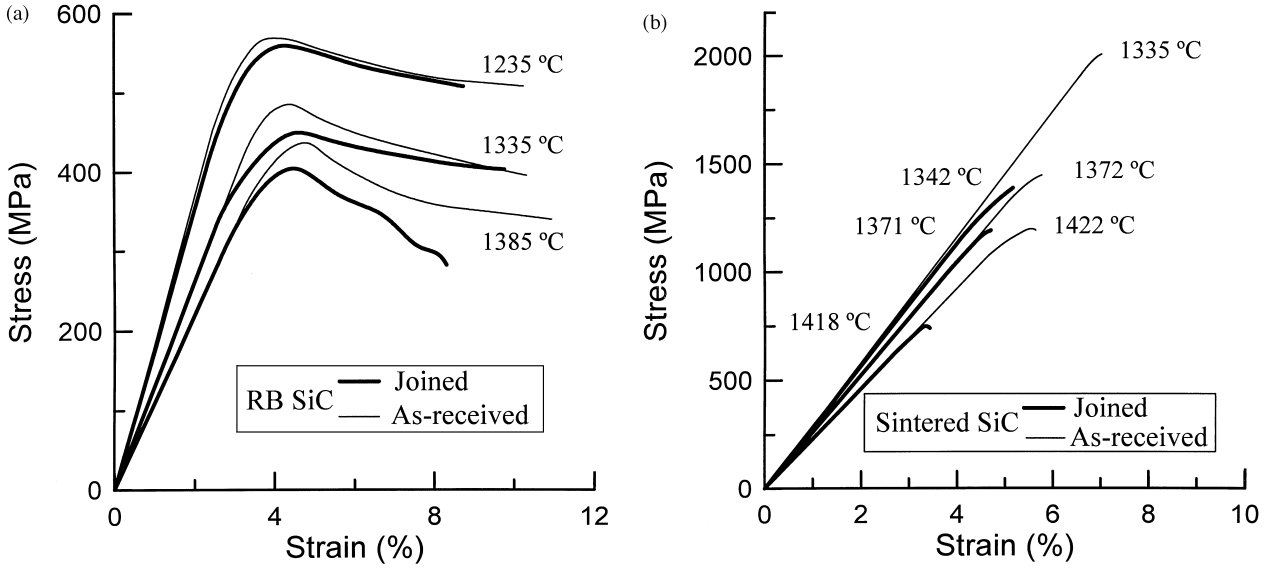

Fig. 6. Plot of stress versus strain as a function of temperatue: (a) for bulk and joined RB-SiC; (b) for bulk and joined sintered SiC.

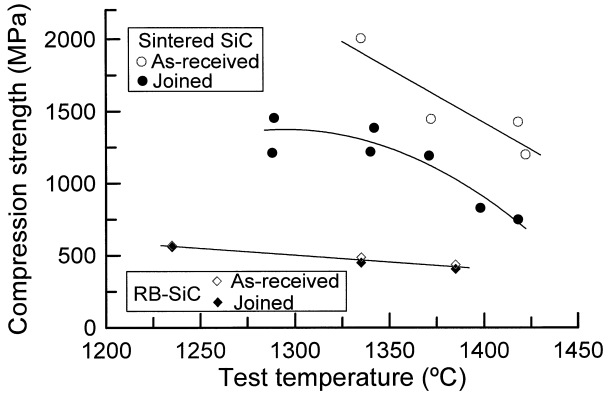

Fig 7. Plot of the maximum strength as a function of temperature. For bulk and joined RB and sintered SiC.

monolithic sintered SiC has higher strength than the joint (associated with the minor amount of intergranular phase in the sintered SiC). For this reason the joint of sintered SiC does not have any appreciable deformation in the pieces joined and the deformation and failure occurs at the joint (Fig. 8b).

The TEM characterization indicates that the joints are well bonded with the bulk material for both types of SiC and that the joint-bulk interphase have not suffered any damage during the joining process, more than the formation of scattered dislocations arrays. For these reasons the joined SiC fails either on the bulk of the joined pieces (RB-SiC) or internally in the joint (sintered SiC) but not in the bulk-joint interphase. This fact is corroborated by the SEM observation of the deformed joints in sintered SiC where it can be observed that, although the sample fails in the joints, some joint material remains glued to the bulk SiC.

The stress applied to the joint must be studied in two separated components. One perpendicular to the joining plane that will induce a compressive deformation on the joint, and a second one on the plane of the joint that will induce a shear deformation of the joint. The contribution to the total strain of the shear deformation of the joint is clearly larger than the contribution of the compressive deformation of the joint in the joints of sintered SiC. In the case of the joints of RB-SiC, the situation is not so clear for the deformations at 1235 and 1335°C. For example, in the test run at 1235°C, the total decrease in length of the sample is 160 μm (4% plastic strain) while the width of the joint has a decrease between 0.5 and 6 μm (the average width being 54.8±2.8 μm). The contribution of the shear deformation of the joint to the total strain is difficult to measure directly, but will account for the strain that is not occurring on the bulk RB-SiC or by compression of the joint.

If the sample fails by shear in the joint, the shear strength will be half of the strength of the sample (we must consider the 45° angle of the joint with the compression axis and the surface of the joint relative to the compression surface). This method of measuring the shear strength is actually more accurate than using bending tests[10,11,15] as in those experiments the stresses applied on the joint have also a component that is separating the parts joined. For this reason the values obtained by bending are lower. Additionally, the geometry of the joint related to the applied stress studied in these experiments is more likely to be used because it has a component that is holding the joint. From the experiments with sintered SiC, the value of the shear strength can be determined as the sample is clearly failing in the joint by shear, but for the RB-SiC samples at 1235 and 1335°C the value obtained must be considered as an underestimation.

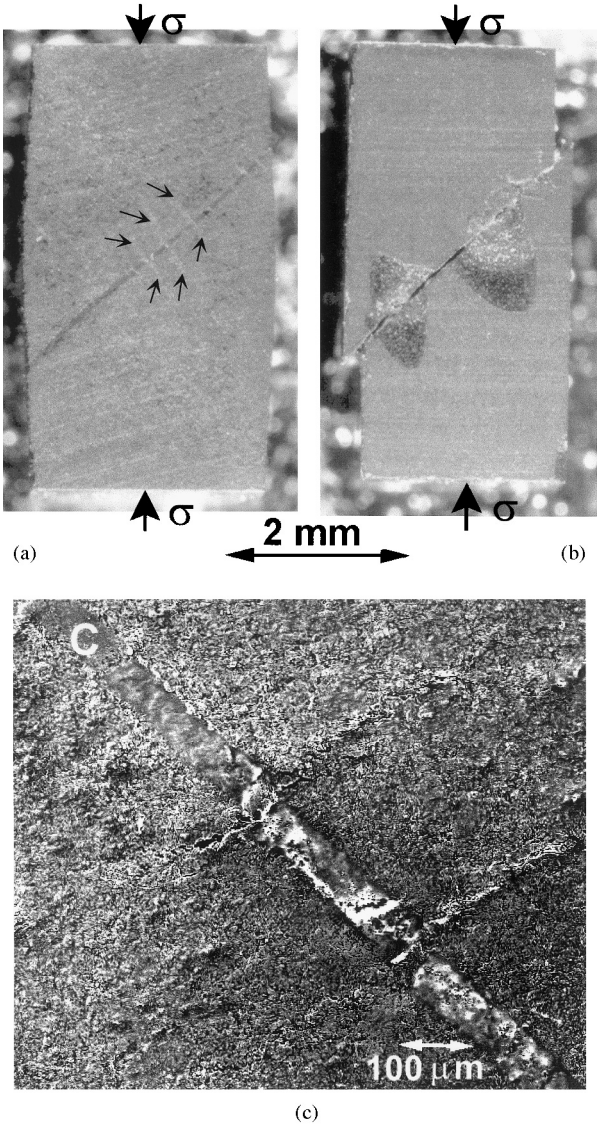

Fig. 8. (a) Optical micrograph of a deformed joint of RB-SiC (deformed at 1235°C); (b) optical micrograph of a deformed joint of sintered SiC (deformed at 1420°C); (c) detail of the zone arrowed on (a).

The strength of the joint is closely related with the active mechanism for plasticity in the joint. One plausible mechanism is viscous flow (which has been successfully applied to systems as Si_3N_4 with intergranular phase of approximately 8 wt.%[16]), in which undeformable SiC grains would move in the silicon matrix, the deformation being controlled by the silicon flow between grain boundaries. The effective viscosity (η) of a system consisting of hard particles embedded in matrix with viscosity (η_o) (for the limit of high particle content) is:[17]

$$\eta = C\frac{\eta_o}{f^3}$$

where f is the volume fraction of viscous phase, and C is a constant ranging from 3 to 11 depending on the geometry of the particles. Considering the viscosity of silicon at the melting point[18] (approximately 10^{-3} Pa s) and taking $f=0.1$, the effective viscosity of the joint would be about 10 Pa s. We can calculate, from the yield stress of the joints, the value of the effective viscosity of the joint considering the relation of the shear stress with the shear strain rate:

$$\sigma_{shear} = \eta\dot{\varepsilon}_{shear}$$

which is about 10^{13} Pa s at 1420°C (over the melting point of silicon) for the joints of sintered SiC. This discrepancy indicates that the SiC grains are actually in contact and they can not move freely without undergoing some plastic deformation. This fact is also supported by the low amount of plasticity that can be supported by the joint. For temperatures under the melting point of silicon, viscous flow is not occurring either. The low creep resistant of silicon at these temperatures[19] (under 10 MPa for similar conditions) is incompatible with a viscous flow model predicting the strengths measured in this work.

It must be taken into account that the joints of the two SiC types are actually deforming at different strain rates. Since the bulk sintered SiC does not deform plastically, all the plastic strain is occurring in the joint (63 μm thick in average). This implies an increase on the strain rate of almost two orders of magnitude compared with the joints of RB-SiC, if the deformation is distributed all along the sample. However, the strength does not increase linearly with strain rate as it would be expected by a viscous model (the strength is only about double or triple in joints of sintered SiC compared to joints of RB-SiC). This means that the strain rate have a power dependence with stress with an exponent over 4. This stress exponent is consistent with creep data from siliconized SiC.[20,21] It is difficult to compare the values of strength versus strain rate obtained in these works with our data because the different range of strain rates (10^{-8} to 10^{-6} versus an effective strain rate of about 10^{-3} s^{-1} in the joints of sintered SiC), but it is consistent with the strength of reaction formed SiC deformed under the same conditions.[22] In siliconized SiC, the plasticity is controlled by the interaction between the SiC grains when the silicon content is low enough. This interaction can result in sliding at the contact sites (when the deformation is done in compression and for deformation at low stress in tension) or cavitation (for deformation at high stress in tension). In the joints studied in this work both mechanisms must be present because the deformation is not in pure compression, and the deformation occurs in the high stress regime define by these authors.[20,21] However, for the temperatures studied, grain boundary sliding accommodation by the plastic deformation of SiC is very limited and the joints fracture after a small strain. The difference in

strength between the bulk sintered SiC, and the joints must be due mainly to the lower volume fraction of SiC in the joint (Carter et al.[23] measured in RB-SiC a creep rate 6 times larger associated with a decrease of 5% on the density).

5. Conclusions

It has been demonstrated that the reaction forming approach can be used to produce strong joints with a uniform microstructure in reaction bonded and sintered silicon carbide materials. The microstructural observations indicated that the joint-SiC interphase is clean without the presence of macroscopic defects. The joint is crystalline and there are preferred orientations between the Si matrix and SiC grains. The nature of the joint-SiC interphase is similar for both types of SiC studied.

The strength of RB-SiC joints is not limited by the joint strength, but by the strength of the bulk (parent) materials. The strength of sintered SiC joints is limited by the joint strength. Due to the low silicon content and microstructure of the joints, the SiC grains can not move freely without undergoing some deformation, resulting in high joint strength comparable to the strength of low silicon content siliconized SiC.

Acknowledgements

The research in Spain was funded by project FEDER 1FD1997-2335. The technical assistance of Mr. R. F. Dacek in this work is greatly appreciated.

References

1. Schwartz, M., *Ceramic Joining*. ASM International, Materials Park, OH, 1990.
2. Nichols, M. G., *Joining of Ceramics*. Chapman and Hall, London, 1990.
3. Messler, R. W., *Joining of Advanced Materials*. Butterworth-Heinemann, Boston, MA, 1993.
4. Fragomeni, J. M. and El-Rahaiby, S. K., *Review of Ceramic Joining Technology* (Report No. 9). Ceramic Information Analysis Center, Purdue University, IN, 1995.
5. Bates, C. H., Foley, M. R., Rossi, G. A., Sandberg, G. J. and Wu, F. J., Joining of non-oxide ceramics for high temperature applications. *Ceramic Bulletin*, 1990, **69**(3), 350–356.
6. Singh, M., Kiser, J. D. and Farmer, S. C., Joining of SiC-based ceramics by reaction forming approach. *Ceram. Eng. Sci. Proc.*, 1997, **18**(3), 161.
7. Singh, M., A reaction forming method for joining of silicon carbide-based ceramics. *Scripta Materialia*, 1997, **37**(8), 1151–1154.
8. Singh, M. and Kiser, J. D., Joining of silicon carbide-based ceramics by reaction forming method. In *Proceedings of Physics & Process Modeling and other Propulsion R&T Conference*, vol. 5. NASA CP-10193, 1997, pp. 1–10.
9. Singh, M., Joining of silicon carbide-based ceramics materials for high temperature applications. *Industrial Heating — J. Thermal Technology*, 1997, **9**, 91–93.
10. Singh, M., Joining of sintered silicon carbide ceramics for high temperature applications. *J. Mater. Sci. Lett.*, 1997, **17**(6), 459–461.
11. Singh, M., Microstructure and mechanical properties of reaction-formed joints in reaction bonded silicon carbide ceramics. *J. Mater. Sci.*, 1998, **33**, 5781–5788.
12. Singh M., A new approach to joining of silicon carbide-based materials for high temperature applications. In *Proceedings of Ceramics: Getting into the 2000's — Part C, Advances in Science and Technology 15,* ed. P. Vincenzini. Techna Srl, Faenza, Italy, 1999, p. 1065.
13. Singh M., Affordable, robust ceramic joining technology (ARCJoinT) for high temperature applications. In *Proceedings of Joining of Advanced and Specialty Materials*. ASM International, Materials Park, OH, 1998, pp. 1–5.
14. Singh, M., Design, fabrication and characterization of high temperature joints in ceramic composites. *Key Engineering Materials*, 1999, **164**, 415–420.
15. Martínez-Fernández J., Valera-Feria F. M. and Singh M., Characterization of microstructure and mechanical properties of joints silicon carbide-based ceramics. In *Proceedings of Joining of Advanced and Specialty Materials*. ASM International, Materials Park, OH, 1998, pp. 35–44.
16. Chadwick, M. M., Jupp, R. S. and Wilkinson, D. S., Creep behavior of a sintered silicon nitride. *J. Am. Ceram. Soc.*, 1993, **76**(2), 385–396.
17. Wilkinson, D. S., Creep mechanisms in multiphase Ceramics Materials. *J. Am. Ceram. Soc.*, 1998, **81**(2), 275–279.
18. Battezzati, L. and Greer, A. L., The viscosity of liquid metals and alloys. *Acta Metall.*, 1989, **37**(7), 1791–1802.
19. Sumino, K., Deformation behavior of silicon. *Metall. Mater. Trans. A*, 1999, **30A**(6), 1465–1479.
20. Chuan, S. T. and Wiederhorn, M., Damage-enhanced creep in a siliconized silicon carbice: mechanics of deformation. *J. Am. Ceram. Soc.*, 1988, **71**(7), 595–601.
21. Wiederhorn, S. M., Roberts, D. E., Chuan, T. and Chuck, L., Damage-enhanced creep in a siliconized silicon carbice: phenomenology. *J. Am. Ceram. Soc.*, 1988, **71**(7), 602–608.
22. Muñoz, A., Martínez Fernández, J., Domínguez Rodríguez, A. and Singh, M., High-temperature compressive strength of reaction-formed silicon carbide (RFSC) ceramics. *J. Eur. Ceram. Soc.*, 1998, **18**, 65–68.
23. Carter, C. H., Davis, R. F. and Bentley, J., Kinetics and mechanisms of high-temperature creep in silicon carbide: I, reaction-bonded. *J. Am. Ceram. Soc.*, 1984, **67**(6), 409–417.